Newly discovered that AH2QDS can be used as a powerful antidote for paraquat: Insight from efficacy observation and RNA-sequencing analysis

Jin Qian
The First Affiliated Hospital of Hainan Medical University
Chun-Yuan Wu
Environment and Plant Protection Research Institute
Dong-Ming Wu
Environment and Plant Protection Research Institute
Li-Hua Li
Hainan Medical University
Qi Li
Hainan Medical University
Tang Deng
The First Affiliated Hospital of Hainan Medical University
Qi-Feng Huang
The First Affiliated Hospital of Hainan Medical University
Shuang-Qin Xu
Hainan Medical University
Hang-Fei Wang
Hainan Medical University
Xin-Xin Wu
Hainan Medical University
Zi-Yi Cheng
Hainan Medical University
Xiao-Ran Liu (hy0203049@hainmc.edu.cn)
The First Affiliated Hospital of Hainan Medical University
Chuan-Zhu Lv
Hainan Medical University

Research Article

Keywords: Paraquat poisoning, Hydroquinone, Detoxify, Oxidative stress

Posted Date: May 4th, 2021

DOI: https://doi.org/10.21203/rs.3.rs-471210/v1

Abstract

Paraquat (PQ) is a widely used fast-acting pyridine herbicide. Accidental ingestion or self-administration via various routes can cause severe organ damage. Currently, no effective antidote is available commercially, and the mortality rate of poisoned patients is exceptionally high. Here, the efficacy of anthrahydroquinone-2-6-disulfonate (AH_2QDS) was observed by us in treating PQ poisoning by constructing in vivo and ex vivo models, we then explored the detoxification mechanism of AH_2QDS. We demonstrated that the PQ concentration in the PQ + AH_2QDS group was significantly reduced compared to that of rat in the PQ group. Besides, AH_2QDS protected the mitochondria of rats and A549 cells and decreased oxidative stress damage, thus improving animal survival and cell viability. Finally, the differentially expressed genes were analysed in the PQ + AH_2QDS group and the PQ group by RNA sequencing, and we verified that Nrf2's expression in the PQ + AH_2QDS group was significantly higher than that in the PQ group. Our work identified the AH_2QDS could reduce functional damage and PQ absorption to organs that are induced by PQ that poisons through direct interaction with PQ. Furthermore, AH_2QDS can protect mitochondria and enhance antioxidative stress injury.

1 Introduction

Paraquat (1,1'-dimethyl-4,4'-bipyridinium, PQ) is a fast-acting herbicide that is widely used for chemical weed control worldwide[1]. PQ is extremely toxic to the human body, with a lethal dose of 5 ~ 15 mL of 20% (w/v) aqueous solution for adults. When PQ enters the body, it is rapidly absorbed and enriched, causing an acute poisoning reaction, so the mortality rate is as high as 50 to 80%[2–4].

The vast majority of PQ poisonings involve oral ingestion, and PQ is rapidly absorbed into the blood via the gastrointestinal tract[5], damaging the digestive tract, kidneys, liver, lungs, and other organs, thus causing multiple organ failure[4]. It is generally believed that PQ causes the formation of abundant reactive oxygen species (ROS) after absorption into the blood[6]. Once an imbalance of the redox system begins to occur, it will destroy mitochondria, causing reduced activity of various antioxidant enzymes, which are continuously stimulated by oxidation in biological systems[7].

Clinically, activated carbon and montmorillonite powder are commonly used via gastric administration, and 20% mannitol is used as a cathartic (“white and black” scheme)[8–10]. The above method is mainly based on the physical adsorption of PQ to accelerate excretion and prevent its further absorption. In addition, many chemical methods for the treatment of PQ poisoning have also been developed, such as vitamin C and glutathione, which are also used to combat peroxidation damage caused by PQ[11,12]. Current anti-PQ therapies include oxygen therapy, immunosuppressants, chemotherapy drugs, antifibrotic drugs, and even lung transplant surgery for the management of PQ poisoning[13–16]. Unfortunately, the clinical benefits of these technologies are insufficient, and the mortality of affected patients remains high. Consequently, a new type of antidote with improved clinical efficacy is still urgently needed.

Recently, we developed an antidote that can directly bind to PQ. This antidote, called anthrahydroquinone-2-6-disulfonate (AH_2QDS), has strong redox properties and can quickly reduce PQ to nontoxic substances in vitro. Since ionic PQ contains a dibasic pyridinium ion structure and AH_2QDS contains a dibasic sulfonic acid structure, both planar structures provide low steric hindrance and strong molecular attraction interactions, which easily leads to the formation of a chain-like structure, with a needle-like structure on a macroscopic scale. Accordingly, PQ can be transformed into a nontoxic substance in the system. Early in vitro experiments found that after mixing PQ with AH_2QDS, a green precipitate was formed immediately. If detoxification is performed at a 1:1 mol ratio, the concentration of PQ in the mixed solution will become zero in a short time. This indicates that AH_2QDS is a specific antidote for PQ.

However, the detoxification effect of AH_2QDS remains to be further studied after PQ poisoning in vivo. Recently, we used A549 cells to establish an in vitro cell line[17]. By detecting mitochondrial membrane potential, observing the microstructure of the cells and detecting cell viability, we proved that compared with the PQ group, the AH_2QDS intervention group showed reduced functional damage of mitochondria and significantly improved cell activity.

To further explore the detoxification mechanism of AH_2QDS, we constructed an SD rat model of PQ poisoning via gavage[5]. Then, we demonstrated that the PQ concentration in the plasma of SD rats detoxified with AH_2QDS was significantly reduced. Furthermore, compared with that in the PQ-treated rats, kidney, lung and liver tissue damage was reduced in the AH_2QDS intervention group. The 30-day survival rate was also improved.

Interestingly, the same trend of antioxidant stress was found in both in vivo and in vitro experiments. That is, in the PQ group, the levels of MDA and ROS increased and the level of GSH-Px decreased, while in the AH_2QDS intervention group, the levels of MDA and ROS decreased and the level of GSH-Px increased. Therefore, we hypothesized that the detoxification mechanism of AH_2QDS is related to antioxidant stress.

To confirm this view, we analysed the differentially expressed genes in lung tissue between the PQ group and the AH_2QDS intervention group by second-generation sequencing, and we found that oxidative stress plays an essential role in AH_2QDS treatment of PQ poisoning and that the nuclear factor Nrf2 plays a vital role in this process. AH_2QDS reduced oxidation products, thereby helping to reduce oxidative damage to protect against PQ poisoning.

In summary, AH_2QDS is a specific antidote for paraquat, it reduces oxidation products, reducing oxidative damage and thereby preventing PQ poisoning.

2 Results

2.1 Binding of PQ and AH_2QDS

First of all, we showed the binding of PQ and AH_2QDS (Fig. 1) utilizing AutoDock Vina. Then, we constructed in vivo and in vitro models to verify the efficacy of AH_2QDS in PQ poisoning.

2.2 AH_2QDS for the treatment of PQ poisoning in vitro

In the in vitro experiment, we first used CCK8 to determine the effects of different concentrations of PQ on the viability of A549 cells[18]. As shown in Figure S1, the cell viability decreased gradually in a time-dependent manner starting 24 h after the PQ intervention. Interestingly, a significant difference in cell viability was caused by different concentrations of PQ at 48 h. At 72 h, under the 300 μM PQ intervention, the cell viability decreased to 50% (Figure S1). According to the data, we used this condition in subsequent experiments. At the same time, we measured the effects of different concentrations of AH_2QDS on the viability of A549 cells (Figure S2A). It is worth noting that when the concentration of AH_2QDS is greater than 200 μM, it will also have a toxic effect on cells, so we chose 200 μM AH_2QDS as the concentration for the follow-up experiment. Given the oxidative damage-related mechanism of PQ, we also used glutathione, which is often used to resist the damage caused by oxidative stress[12]. Here, we chose different concentrations of glutathione to determine its effect on the viability of A549 cells (Figure S2B). The results showed that glutathione had no toxic effect on cells.

Next, Fig. 2A-B showed that PQ could significantly reduce the viability of A549 cells, while both glutathione and AH_2QDS showed protective effects on A549 cells. Interestingly, the protective effect of our antidote AH_2QDS was more potent than that of glutathione, suggesting that AH_2QDS may have more powerful antioxidant activity.

2.3 AH_2QDS improve antioxidation in the treatment of PQ poisoning

PQ poisoning often causes oxidative stress damage. Consistent with the literature, Our results in Fig. 3A-C showed that the level of GSH-Px in the PQ group decreased, indicating that its antioxidant capacity decreased[19]. In contrast, ROS and MDA levels increased in the PQ group, indicating that oxidative damage was aggravated[20,21]. In this context, the level of GSH-Px in the group treated with AH_2QDS was significantly higher, and the levels of ROS and MDA were significantly lower than those in the PQ group. The same trend was also confirmed in vivo (Fig. 7D-F). In summary, AH_2QDS plays an antioxidant role in the treatment of severe PQ.

2.4 Protective effect of AH_2QDS on cell mitochondria

Many studies have reported that PQ poisoning often causes damage to mitochondria[22–24]. To explore whether AH_2QDS can protect mitochondria, we used a transmission electron microscope to observe the mitochondrial structure under a microscope. From the Fig. 8D-F, we can see that after PQ intervention, the

mitochondrial structure of A549 cells was destroyed, vacuoles appeared in the cell body, the cell wall was broken, and a large number of organelles were extruded. However, the morphology of cells in the control group and PQ + AH_2QDS group was normal, the chromatin was evenly distributed, the morphology of the cells was as expected, and the morphology of the mitochondria was normal. Furthermore, through detection of the mitochondrial membrane potential, we found that the membrane potential of the PQ + AH_2QDS high-dose group was the highest, followed by the high-dose group and PQ + AH_2QDS low-dose group, and the mitochondrial membrane potential of the PQ group was the lowest (Fig. 3D-H). The above results indicate the protective effect of AH_2QDS on cell mitochondria in vitro.

2.5 The survival rate in a rat model of hyperlethal PQ poisoning

In this study, to determine PQ toxicity, we intragastrically administered PQ at doses of 100, 200, 300, 400, and 500 mg/kg in vivo (Figure S3A). We found that when the concentration of PQ was more than 200 mg/kg, the rats showed obvious poisoning symptoms and began to die. When the concentration of PQ was more than 300 mg/kg, all the animals died within two weeks. When the concentration of PQ was more than 400 mg/kg, the animals died in approximately three days. According to these data, we chose 400 mg/kg (a hyperlethal dose) as the dose of PQ to evaluate the detoxification effect of AH_2QDS. Subsequently, we used AH_2QDS to detoxify the animals at different times after exposure. As shown in Fig. 3A, the 30-day survival rate of rats exposed to 400 mg/kg PQ could reach 100% when they were detoxified with AH_2QDS within 2 h. However, as the time window for AH_2QDS treatment was extended, the 30-day survival rate of SD rats gradually decreased (Figure S3B). According to the above results, we chose 2 h as the detoxification time of AH_2QDS. Next, we designed different experimental groups to verify the detoxification effect of AH_2QDS (Fig. 4B). We discovered that the control group's 30-day survival rates, the AH_2QDS group, and the PQ + AH_2QDS group were all 100%. The control group's 30-day survival rates and the PQ + conventional therapy group were zero, and all of the rats died within one week. The detoxification effect of AH_2QDS is better than that of the “white and black” scheme.

2.6 AH_2QDS reduces organ damage in a rat model of PQ poisoning

The lung is the main target organ after PQ poisoning[25]. Patients often die of acute lung injury in the early stage, and pulmonary fibrosis often occurs later[26,27]. According to Fig. 5A-P, we also observed alveolar inflammation in the lung tissue of rats in the PQ and PQ + conventional therapy groups at all time points, including destruction of the alveolar structure, oedema in the alveolar cavity, intracapillary hyperaemia, and inflammatory cell infiltration, indicating acute lung injury. On the seventh day, alveolar fusion, alveolar septum thickening, and fibrous tissue hyperplasia were found in the lungs of the two groups, indicating pulmonary fibrosis. However, the lung tissues of rats in the control, AH_2QDS, and PQ + AH_2QDS groups were as expected at all periods, with very little infiltration of inflammatory cells, no collapse of the

alveolar walls, no thickening of the alveolar septa, no exudation in the alveoli, and no capillary dilation, hyperaemia or other manifestations. The pathological injury score of the lung tissue showed that lung injury in the PQ group and PQ + conventional therapy group was significantly worse than that in the control, AH_2QDS, and PQ + AH_2QDS groups, and the difference was statistically significant ($p < 0.001$) (Fig. 5Q).

In addition to lung injury, PQ poisoning can also cause severe functional damage to multiple organs, so we measured the liver and kidney function and blood gas of the SD rats in each group[28–30]. As shown in Fig. 6A-B, the ALT, AST, CREA, and UREA levels in the PQ and PQ + conventional therapy groups increased from the 3rd day and peaked on the 7th day. The ALT, AST, CREA, and UREA levels in the control, AH_2QDS, and PQ + AH_2QDS groups were significantly lower than those in the PQ and PQ + conventional therapy groups in the first seven days, and the difference was statistically significant ($P < 0.001$). In addition, we compared the PQ group with the PQ + conventional therapy group and found that the ALT, AST, CREA, and UREA levels in the PQ + conventional therapy group were significantly lower than those in the PQ group ($P < 0.001$). However, the hepatic and renal function of the control, AH_2QDS, and PQ + AH_2QDS groups was in the normal range during each period, and there was no significant difference between them ($P > 0.05$). PQ poisoning has been verified to cause functional damage to multiple organs, and AH_2QDS treatment of PQ poisoning can reduce liver and kidney function damage. The blood gas analysis results showed (Fig. 6C-D) that the pH and PaO2 values in the PQ and PQ + conventional therapy groups were significantly lower than those in the control, AH_2QDS, and PQ + AH_2QDS groups ($P < 0.001$). Compared with the PQ group and PQ + conventional therapy group, the pH and PaO2 values in the PQ + conventional therapy group were significantly higher than those in the PQ group. The PaO2 values in the control, AH_2QDS, and PQ + AH_2QDS groups were in the normal range during each period, and there was no significant difference between the three groups ($P > 0.05$). Contrary to this trend, the PaCO2 values in the PQ and PQ + conventional therapy groups showed an increasing trend, indicating that hypoxaemia and carbon dioxide retention occurred in PQ-poisoned rats, which eventually led to type II respiratory failure. In summary, these findings suggest that AH_2QDS can reduce the damage to organ function caused by PQ poisoning.

2.7 AH_2QDS can rapidly reduce the concentration of PQ in vivo

As shown in Fig. 7A-C, the PQ concentration in the PQ group peaked at 4 h and decreased to 0 at 96 h. The concentration of PQ in the PQ + AH_2QDS group and PQ + conventional therapy group decreased immediately after 2 h and was significantly lower than that in the PQ group ($P < 0.001$). The difference between 2 h and 24 h was significantly smaller in the PQ + AH_2QDS group than in the PQ + conventional therapy group, and the difference was statistically significant. Similarly, the concentration of PQ in the lung tissue and urine decreased significantly in the PQ + AH_2QDS group. The decrease in PQ drug concentration may have occurred because AH2QDS neutralizes PQ in the gastrointestinal tract.

2.8 Protection of mitochondria by AH_2QDS in vivo

The induction of mitochondrial damage by PQ has been confirmed in in vitro experiments, and we also observed the same phenomenon in vivo experiments. Figure 8B showed that the PQ group's mitochondria were swollen, structurally damaged, vacuolated and empty. Under the electron microscope, the mitochondrial structure was as expected in the rat lung tissues in the control group and PQ + AH_2QDS group (Fig. 8A/C). These pictures illustrated that AH_2QDS protects the structure of mitochondria.

2.9 RNA sequencing

As illustrated in the Figure S4, in this experiment, different samples from the same experimental group are arranged compactly and aggregated into clusters, showing good repeatability. In contrast, different experimental groups are clearly separated from each other, showing reasonable specificity. From the PCA results, the experimental data of this case are fully reliable and of high quality[31]. We can see from Fig. 9A that there were 3325 gene changes in the PQ group compared with the PQ + AH_2QDS group, including 1455 upregulated genes and 1870 downregulated genes. As shown in Fig. 9B, the most differentially regulated pathways in these two samples are the PI3K-AKT pathway, MAPK pathway, AMPK pathway, etc. Consistent with our previous findings, these pathways are mainly oxidative stress-related pathways. We investigated the most significant pathway, namely, the PI3K-AKT pathway, to identify the genes with significant changes, and the results showed that Nrf2, Foxo3, Rxra, Itga4, Creb3l2, Angpt1, Egfr, Tnc, Lamc1, and Met were significantly upregulated. Nrf2 is significantly upregulated in tissues, and its function is closely related to oxidative stress, so we speculate that Nrf2 may be an essential gene for AH_2QDS treatment of PQ poisoning.

We further verified by western blot and RT-qPCR experiments that in in vitro experiments, as illustrated in the Fig. 10A-C, compared with PQ treatment, glutathione and AH_2QDS could significantly increase the expression of Nrf2, while the Nrf2 level of PQ + AH_2QDS group was significantly higher than that of the PQ + glutathione group. The in vivo experiment showed that the levels of Nrf2 in the AH_2QDS, PQ, and PQ + conventional therapy groups were higher than that in the control group, while the Nrf2 level in the PQ + AH_2QDS group was significantly higher than those in the other groups (Fig. 10D-F). The results indicated that conventional therapy (“white and black” scheme) did not activate Nrf2. In contrast, glutathione could increase the expression of Nrf2, but its effect was weaker than that of AH_2QDS, indicating that our antidote, AH_2QDS, could significantly increase the expression of Nrf2, thus exerting its detoxification effect.

3 Discussion

In this study, we used AH_2QDS as an intervention in a model of PQ poisoning. Compared with those of the PQ group, the poisoning symptoms of the PQ + AH_2QDS group were significantly improved, with a lower blood drug concentration, less organ function damage, and a higher survival rate. In the PQ +

AH_2QDS group, mitochondrial damage in lung tissue was alleviated, and a similar phenomenon was found in the cell test. The structure of the mitochondria was intact, the damage was significantly alleviated, and the expression of Nrf2 was significantly increased. These studies have proven for the first time that AH_2QDS is an effective treatment for PQ poisoning, and Nrf2 plays a crucial role in its detoxification process.

Previous studies have shown that activated carbon or the “white and black” scheme can effectively treat PQ poisoning[8–10]. In contrast, our experiments only confirmed that the use of the conventional “white and black” scheme can quickly and effectively reduce the PQ blood concentration but does not affect the survival rate of rats. On the one hand, a superlethal dose of PQ was used to construct the poisoning model, and the drug intervention time was as long as 2 h, during which most of the PQ may have been absorbed into the blood, while the “white and black” scheme could only absorb the residual poison in the stomach and accelerate its excretion but had no effect on the PQ already in the blood. On the other hand, the results also showed that AH_2QDS is not only faster than the “white and black” scheme in removing toxins but also plays a specific role in the blood-related effects of PQ.

The toxic effect of PQ on mitochondria was proposed as early as 1968[32]. Since then, a large number of studies on the damage of PQ to mitochondria have been published[22–24]. Some scholars indicated that PQ could cause accumulation of the hMn-SOD precursor of human manganese-dependent peroxidase and reduce Mn-SOD activity. The conversion of GSH to GSSG leads to a decrease in GSH levels and weakens its antioxidant activity[33]. Other studies have shown that PQ can cause the production of H2O2 and reduce the activity of catalase[34]. H2O2 can induce changes in mitochondrial permeability and affect the mitochondrial membrane potential, resulting in the movement of cytochrome C from the mitochondria into the cytoplasm, and then induce apoptosis by activating caspase9[35]. In our study, the microstructure of the lung tissue and A549 cells in the PQ group was observed under a projection electron microscope. It was found that the structure of the mitochondria was destroyed, vacuoles appeared in the cells, the cell walls were broken, and a large number of organelles were extruded. In contrast, the morphology of the mitochondria in the PQ + AH_2QDS group was as expected, and the lamellar structure was normal. The cell membrane potential of the PQ + AH_2QDS high-dose group was the highest, and the membrane potential was positively correlated with the concentration of AH_2QDS, while the mitochondrial membrane potential of cells treated with only PQ was the lowest. In summary, PQ can destroy the tissue structure of the mitochondria, affect the membrane potential, and eventually lead to cell rupture and death, while AH_2QDS can prevent this process and protect the function and structure of the mitochondria.

The data show that after PQ is absorbed into the blood, it causes the formation of excess reactive oxygen species (ROS), which leads to imbalance of the redox system, the consumption of NADPH, damage to mitochondria, the destruction of lipids, proteins and DNA, and a decrease in the activity of various antioxidant enzymes[20]. After continuous oxidative stimulation, the body eventually sustains tissue damage. A large amount of ROS produced by PQ may be the leading cause of acute lung injury caused by PQ poisoning. In this study, it was found that after PQ exposure, the levels of ROS and MDA in the PQ

group and conventional treatment group increased, while the level of GSH-Px decreased. In the PQ + AH_2QDS group, the ROS and MDA levels decreased, and the level of GSH-Px increased. The results show that PQ can produce a large amount of ROS to cause lipid peroxidation and oxidative stress injury. AH_2QDS can inhibit PQ's effect, improve antioxidant ability, and reduce the level of lipid peroxidation.

After further investigation of the detoxification mechanism of AH_2QDS, we found that the main differentially regulated pathway was the oxidative stress pathway, in which we found that the nuclear factor Nrf2 was significantly upregulated. Many studies have shown that Nrf2 can be used as a "guard" to protect the body against a variety of toxic effects[36–38]. Nrf2 can be activated in a variety of processes involving oxidative stress. Nrf2 was expressed in epithelial cells, macrophages and vascular endothelial cells of normal rat lung tissue[39–41]. MDA in the serum of rats poisoned by PQ increased significantly with the prolongation of poisoning time, while the activity of SOD decreased significantly. Nrf2 protein increased significantly in lung tissue injury induced by PQ. It has been found that the Nrf2-ARE pathway protects the lungs against dibutyl hydroxytoluene-induced acute respiratory distress syndrome (ARDS) and hyperoxia-induced lung injury by activating antioxidant enzymes[42,43]. In our experiment, PQ, as a potent stressor, could activate the Nrf2 signalling pathway. Nrf2 was expressed at low levels in normal rat lung tissue and A549 cells, but the expression of Nrf2 was significantly increased after AH_2QDS treatment. These results show that Nrf2 plays a vital role in the treatment of PQ poisoning by AH_2QDS.

The direct mechanism of AH_2QDS in the treatment of PQ poisoning is that AH_2QDS enters the gastrointestinal tract and comes into contact with the PQ solution. Through a rapid redox reaction, PQ is reduced to a nontoxic green needle-like solid. Thus, detoxification is realized. Energy spectrum analysis showed that the acicular substance was stable and could not be dissolved in strong acids, strong bases, or organic solvents and was extremely stable at room temperature and pressure. At the same time, it was also found in the faeces of SD rats. We were concerned that after administration of AH_2QDS, a green needle-like solid will be formed in the blood, leading to the formation insoluble thrombi and resulting in thrombotic disease and a series of clinical symptoms. Therefore, we tested the blood and tissues of experimental animal SD rats but did not find this substance. So, after administering AH_2QDS, green needle-like solids would not be formed in the blood, tissues and organs to cause thrombotic disease.

To prove whether there is an indirect mechanism of AH_2QDS in PQ poisoning treatment, we constructed animal and cell models. ELISA, WB, and qPCR were performed to detect the levels of GSH-Px, MDA, ROS, and Nrf2, and transmission electron microscopy was performed to observe the microstructure of the mitochondria. The same trend was observed in vivo and in vitro. After the intervention with AH_2QDS, the expression of nuclear factor Nrf2 was enhanced, mitochondrial damage was reduced, and antioxidant stress was improved. Unfortunately, our experiment cannot determine whether the mechanism of AH_2QDS in the treatment of PQ poisoning is the direct mechanism or the indirect mechanism. Further research is needed.

In this paper, AH_2QDS was used as an antidote in the treatment of PQ poisoning for the first time and achieved excellent results, but this was verified only in SD rats, and it has not been tested in more advanced mammals; thus, a long and strict clinical study is needed to investigate the use of AH_2QDS in humans. Additionally, a superlethal dose of PQ was given to SD rats in the poisoning model, and AH_2QDS was given for detoxification 2 hours later. The 30-day survival rate of SD rats in the treatment group reached 100%, but if the time window of treatment with AH_2QDS were prolonged (2.5 h, 3 h, 4 h, or 6 h), the 30-day survival rate of SD rats in the treatment group decreases with the prolongation of intervention time. This may be because 2 h after ingestion of PQ, the rats have rapidly absorbed it into the blood and transported it to various organs through the blood flow. Even if AH_2QDS can detoxify the absorbed PQ, too high a concentration of PQ causes irreversible toxic damage to the organs in this time. In the follow-up studies, the sequencing results will be further analysed, and mechanistic research will be performed to elucidate the molecular functions of the gene, the cell location, and the biological process involved. At the same time, experiments were carried out on the Nrf2-ARE pathway through gene silencing/overexpression of related proteins to demonstrate the profound relationship between the Nrf2-ARE pathway and AH_2QDS in the treatment of PQ poisoning.

In summary, this study verified the therapeutic effect of AH_2QDS on PQ poisoning and explored its mechanism. The relationship between mitochondrial damage, the expression changes upstream and downstream of the Nrf2-ARE pathway, and AH_2QDS in PQ poisoning treatment needs to be further explored.

4 Methods

4.1 Animals and cell lines

All animal experiments were performed as per the protocols approved by the Animal Care and Use Committee of Hainan Medical University. All methods were performed in accordance with the guidelines and regulations of the Animal Care and Use Committee of Hainan Medical University and as per the ARRIVE guidelines 2.0. Human type II alveolar lung epithelial cells (A549) were purchased from the Shanghai Institute for Biological Sciences. The cells were maintained in a 5% CO2 incubator at 37°C in medium (F12K) supplemented with 10% FBS and penicillin/streptomycin (100 U/ml). Sprague-Dawley (SD) rats (8 weeks, male, SPF grade) were purchased from Changsha Tianqn Biotechnology Co., Ltd., and were maintained in specific pathogen-free (SPF) facilities.

4.2 Main reagent

Paraquat solution, purchased from Nanjing Red Sun Co., Ltd., was given at a 400 mg/kg concentration. Twenty percent PQ solution was diluted into 1 mL of PQ solution with PBS. For the “white and black” scheme, 500 mg/kg activated carbon, 500 mg/kg montmorillonite powder and 5 mL mannitol were used for gastric cancer. Activated carbon was purchased from National Pharmaceutical Group Chemical Reagent Co., Ltd. Montmorillonite powder was purchased from Xiansheng Pharmaceutical Co., Ltd.

Mannitol (20%) was purchased from Jiangsu Zhengda Tianqing Pharmaceutical Co., Ltd. Anthrahydroquinone-2-6-disulfonate (AH_2QDS) was synthesized by the Chinese Academy of Tropical Agricultural Sciences. The method is patented (Patent No: 2016103413306). Chemical name: anthraquinone-2-dioxo-6-disodium disulfonate, chemical formula: C14H8O8S2.2Na, molecular weight: 368.33. We prepared the AH_2QDS solution at a concentration of 40 mmol/L.

4.3 Modeling studies of PQ and AH_2QDS binding

Chemical structures of PQ and AH_2QDS were drawn with ChemDraw Pro 16.0 software. The binding conformations between PQ and AH_2QDS were simulated with AutoDock Vina[5].

4.4 Cell Counting Kit-8 (CCK8)

A549 cells were incubated with different concentrations of PQ, AH_2QDS and glutathione for 12 h. After 12, 24, 48 and 72 h, 10 μL of CCK8 solution (Dojindo, Japan) was added, and the cells were incubated in the incubator for 2 h. An enzyme labelling instrument was used to measure the absorbance at 450 nm, and a formula was used to calculate the cell viability.

4.5 Mitochondrial membrane potential

The cell culture medium was removed, the cells were washed with PBS, 1 ml of medium was added, and 1 mL of JC-1 staining working solution was added and mixed well. After incubating the cells for 20 min in the incubator at 37℃, the supernatant was removed, the cells were washed with diluted staining buffer (1x), 2 mL of medium was added, and images were captured under the fluorescence microscope.

4.6 Animal experiments

SD rats (~ 300 g) were subjected to intragastric administration of 400 mg/kg PQ, and 500 mg/kg "white and black" scheme and 400 mg/kg AH_2QDS intervention treatment were administered 2 h later. The specific methods used to establish the model is shown in Fig. 4A. We selected rats without collecting blood after establishing the model and observed and recorded the survival of each group over 30 days. The occurrence of death was recorded as 1, and no death was recorded as 0. Finally, a survival curve was drawn. The experiment was carried out according to the guiding principles for animal experiments at Hainan Medical University.

4.7 Sample collection

Blood was collected from the rats at different time points in anticoagulant tubes treated with heparin, and the plasma was separated and stored at -80°C for the detection of drug concentrations in the blood. The urine was left in the centrifuge tube for the detection of drug concentrations in urine. Rats were anaesthetized by intraperitoneal injection of 10% chloral hydrate (300 mg/kg), and the blood from the abdominal aorta was collected for the detection of liver, kidney and lung function. Finally, the rats were killed by exsanguination, and the lung tissue was collected, washed with PBS and stored at -80°C for follow-up analysis. The bodies of the animals were then incinerated.

4.8 Histopathology

SD rats were sacrificed at different times, and the lungs of the rats were harvested, fixed in 4% formalin, embedded in paraffin, sectioned, and stained with haematoxylin and eosin (H&E). The lung injury score was determined according to methods that were previously reported in the literature[44].

4.9 Blood analysis

The collected venous blood samples were placed into a test tube with a coagulant and centrifuged at 3000 r/min for 5 minutes. Rat serum was obtained and placed into an automatic biochemical function analyser for analysis. After collecting blood from the abdominal aorta with an arterial blood gas sampler and rubbing with both hands for 1 minute, 0.1 mL was injected into the blood gas analyser for analysis.

4.10 Transmission electron microscopy

Lung tissue and A549 cells were collected and placed overnight in 2.5% glutaraldehyde fixed solution that was prechilled at 4°C, cleaned with PBS, fixed with 1 ml of 1% osmic acid for 1.5 h, dehydrated with alcohol and acetone, and impregnated with resin, and ultrathin sections were stained with uranium acetate and lead citrate. The ultrastructure was observed under a transmission electron microscope.

4.11 Ultra-high-performance liquid chromatography-tandem mass spectrometry

The concentrations of PQ and AH_2QDS were determined by ultra-high-performance liquid chromatography-tandem mass spectrometry (UPLC/Xevo TQ-S, Waters). The mobile phase was acetonitrile/100 mM ammonium formate (pH = 3.7) = 50 × 50, and the flow rate was 0.3 mL/min. An ACQUITY UPLC BEH HILIC column (100 mm × 2.1 mm, 1.7 μm) was used. PQ was quantified in the MRM mode of positive ion multireaction monitoring with an electrospray ion source. Negative ion SIR mode was used to quantify AH_2QDS. The parameters were as follows: capillary voltage: 3.2 kV, ion source temperature: 150°C, cone hole back blowing gas flow rate: 30 L/hr, dissolvent temperature: 350°C, and dissolvent gas flow rate: 800 L/hr.

4.12 Cytokine detection

The GSH-Px, MDA and ROS kits purchased from Nanjing Jiancheng Company were used according to the instructions to detect the levels of GSH-Px, MDA and ROS, respectively.

4.13 Western blotting

Proteins were extracted from tissues and cells with a BCA kit (Biyuntian Biotechnology Co., Ltd.), separated in SDS-PAGE gels, and transferred to cellulose membranes. After sealing, the membranes were incubated with the primary antibody overnight, then incubated with the secondary antibody for 1 h (Table S1), and finally developed by exposure.

4.14 Quantitative real-time polymerase chain reaction (RT-qPCR)

TRIzol (Biyuntian Biotechnology Co., Ltd.) was used to extract RNA, and a cDNA reverse transcription kit (Applied Biosystems, cat. no. 4368814) was used to reverse-transcribe the extracted RNA into cDNA. PCR was performed on an ABI Prism 7900HT system (Applied Biosystems, Foster City, CA, USA) using SYBR GREEN PCR Master Mix (Applied Biosystems). Primers were purchased from Sangon Biotech (Shanghai) Co., Ltd. The primer sequences are listed in Table S2.

4.15 RNA-sequencing

Total RNA was extracted from the samples, and magnetic beads were used to enrich eukaryotic mRNA. Fragmentation buffer was added to the mRNA as a template, the first cDNA strand was synthesized with six-base random primers (random hexamers), and buffer, dNTPs, RNase H and DNA polymerase I were added to synthesize the second cDNA strand. After purification with a QiaQuick PCR kit and elution with EB buffer, terminal repair was performed, poly (A) was added, the sequencing connector was connected, and the fragment size was selected by agarose gel electrophoresis and PCR amplification. The sequenced library was sequenced with Illumina HiSeq sequences. The data obtained by sequencing on the Illumina platform were used for quality control (QC). Raw reads were filtered to obtain clean reads, and the clean reads were compared to the reference sequence. Statistical analysis of the distribution and coverage of reads on the reference sequence, the second quality control step (QC of alignment), as well as gene expression, screening of differentially expressed genes among samples, and significant enrichment analysis of KEGG pathways were completed by Nextomics Biosciences Co., Ltd.

4.16 Statistical analysis

Statistical analyses were performed using GraphPad Prism 8.0 or SPSS 20.0 software. Measurement data are expressed as the mean ± SEM, and significance was tested by single-factor analysis of variance (ANOVA). Kaplan-Meier survival analysis was used to analyse the survival rate of rats in different treatment groups. $P < 0.05$ indicates that a difference is statistically significant.

Declarations

6 Acknowledgements

This project supported by Hainan Province Key R&D Program (ZDYF2019125), National Natural Science Foundation of China (81960351), and Hainan Provincial Natural Science Foundation of China (820QN398). We would like to thank the Science experiment Center of Hainan Medical College for providing a venue for our experiment.

7 Author contributions

JQ, CYW and DMW carried out experimental analysis on the data and drafted the manuscript. LHL, QL, TD, QFH, SQX, HFW and XXW performed the statistical analysis. ZYC, XRL and CZL conceived of the study, and participated in its design and coordination and helped to draft the manuscript. All authors read and approved the final manuscript.

8 Additional Information

The experiment was carried out according to the guiding principles for animal experiments at Hainan Medical University.

9 Competing interests

The authors have declared that no competing interest exists.

References

1 Cicchetti, F., Drouin-Ouellet, J. & Gross, R. E. Environmental toxins and Parkinson's disease: what have we learned from pesticide-induced animal models? *Trends Pharmacol Sci***30**, 475-483, doi:10.1016/j.tips.2009.06.005 (2009).

2 Wu, W.-P. *et al.* Addition of Immunosuppressive Treatment to Hemoperfusion Is Associated with Improved Survival after Paraquat Poisoning: A Nationwide Study. *PLOS ONE*, doi:10.1371/journal.pone.0087568 (2014).

3 Hong, S. Y., Lee, J. S., Sun, I. O., Lee, K. Y. & Gil, H. W. Prediction of patient survival in cases of acute paraquat poisoning. *PLoS One***9**, e111674, doi:10.1371/journal.pone.0111674 (2014).

4 Gawarammana, I. B. & Buckley, N. A. Medical management of paraquat ingestion. *Br J Clin Pharmacol***72**, 745-757, doi:10.1111/j.1365-2125.2011.04026.x (2011).

5 Zhang, X. *et al.* A Synthetic Receptor as a Specific Antidote for Paraquat Poisoning. *Theranostics***9**, 633-645, doi:10.7150/thno.31485 (2019).

6 Dinis-Oliveira, R. J. *et al.* Paraquat Poisonings: Mechanisms of Lung Toxicity, Clinical Features, and Treatment. *Critical Reviews in Toxicology***38**, 13-71, doi:10.1080/10408440701669959 (2008).

7 Tsukamoto, M., Tampo, Y., Sawada, M. & Yonaha, M. Paraquat-Induced Oxidative Stress and Dysfunction of the Glutathione Redox Cycle in Pulmonary Microvascular Endothelial Cells. *Toxicology and Applied Pharmacology***178**, 82-92, doi:https://doi.org/10.1006/taap.2001.9325 (2002).

8 Feng, E., Cheng, Y., Tan, Z. & Wang, H. [Experience of continuous fluid therapy in successfully rescuing a patient with acute severe paraquat poisoning]. *Zhonghua wei zhong bing ji jiu yi xue***31**, 1043-1044, doi:10.3760/cma.j.issn.2095-4352.2019.08.027 (2019).

9 Wang, W. *et al.* [Effect of rhubarb as the main composition of sequential treatment in patients with acute paraquat poisoning: a prospective clinical research]. *Zhonghua wei zhong bing ji jiu yi xue***27**, 254-258, doi:10.3760/cma.j.issn.2095-4352.2015.04.006 (2015).

10 Zhao, B. *et al.* [Clinical study on the treatment of acute paraquat poisoning with sequential whole gastric and bowel irrigation]. *Zhonghua lao dong wei sheng zhi ye bing za zhi = Zhonghua laodong weisheng zhiyebing zazhi = Chinese journal of industrial hygiene and occupational diseases***33**, 213-215 (2015).

11 Rodrigues da Silva, M. *et al.* Beneficial effects of ascorbic acid to treat lung fibrosis induced by paraquat. *PloS one***13**, e0205535, doi:10.1371/journal.pone.0205535 (2018).

12 Kobayashi, S. *et al.* Enhanced expression of cystine/glutamate transporter in the lung caused by the oxidative-stress-inducing agent paraquat. *Free radical biology & medicine***53**, 2197-2203, doi:10.1016/j.freeradbiomed.2012.09.040 (2012).

13 Lin, X. *et al.* Association between liberal oxygen therapy and mortality in patients with paraquat poisoning: A multi-center retrospective cohort study. *PloS one***16**, e0245363, doi:10.1371/journal.pone.0245363 (2021).

14 Li, L., Sydenham, E., Chaudhary, B., Beecher, D. & You, C. Glucocorticoid with cyclophosphamide for paraquat-induced lung fibrosis. *The Cochrane database of systematic reviews*, CD008084, doi:10.1002/14651858.CD008084.pub4 (2014).

15 Gawarammana, I. *et al.* High-dose immunosuppression to prevent death after paraquat self-poisoning - a randomised controlled trial. *Clinical toxicology (Philadelphia, Pa.)***56**, 633-639, doi:10.1080/15563650.2017.1394465 (2018).

16 Pourgholamhossein, F. *et al.* Pirfenidone protects against paraquat-induced lung injury and fibrosis in mice by modulation of inflammation, oxidative stress, and gene expression. *Food and chemical toxicology : an international journal published for the British Industrial Biological Research Association***112**, 39-46, doi:10.1016/j.fct.2017.12.034 (2018).

17 Ariyama, J., Shimada, H., Aono, M., Tsuchida, H. & Hirai, K. Propofol improves recovery from paraquat acute toxicity in vitro and in vivo. *Intensive care medicine***26**, 981-987, doi:10.1007/s001340051291 (2000).

18 Zhang, D. *et al.* Role of AP-2alpha and MAPK7 in the regulation of autocrine TGF-beta/miR-200b signals to maintain epithelial-mesenchymal transition in cholangiocarcinoma. *J Hematol Oncol***10**, 170, doi:10.1186/s13045-017-0528-6 (2017).

19 Liu, Z., Wang, X., Li, L., Wei, G. & Zhao, M. Hydrogen Sulfide Protects against Paraquat-Induced Acute Liver Injury in Rats by Regulating Oxidative Stress, Mitochondrial Function, and Inflammation. *Oxidative medicine and cellular longevity***2020**, 6325378, doi:10.1155/2020/6325378 (2020).

20 Zhang, Z. *et al.* Klotho Alleviates Lung Injury Caused by Paraquat via Suppressing ROS/P38 MAPK-Regulated Inflammatory Responses and Apoptosis. *Oxidative medicine and cellular longevity***2020**,

1854206, doi:10.1155/2020/1854206 (2020).

21 Ma, J., Li, Y., Li, W. & Li, X. Hepatotoxicity of paraquat on common carp (Cyprinus carpio L.). *The Science of the total environment*, 889-898, doi:10.1016/j.scitotenv.2017.10.231 (2018).

22 Xie, L. *et al.* SIRT3 Mediates the Antioxidant Effect of Hydrogen Sulfide in Endothelial Cells. *Antioxidants & redox signaling***24**, 329-343, doi:10.1089/ars.2015.6331 (2016).

23 Bora, S. *et al.* Paraquat exposure over generation affects lifespan and reproduction through mitochondrial disruption in C. elegans. *Toxicology***447**, 152632, doi:10.1016/j.tox.2020.152632 (2021).

24 Wang, X., Souders, C., Zhao, Y. & Martyniuk, C. Paraquat affects mitochondrial bioenergetics, dopamine system expression, and locomotor activity in zebrafish (Danio rerio). *Chemosphere***191**, 106-117, doi:10.1016/j.chemosphere.2017.10.032 (2018).

25 Jin, Y. *et al.* Transplantation of endothelial progenitor cells attenuated paraquat-induced acute lung injury via miR-141-3p-Notch-Nrf2 axis. *Cell Biosci***8**, 21, doi:10.1186/s13578-018-0219-1 (2018).

26 Wu, L. *et al.* Metformin Activates the Protective Effects of the AMPK Pathway in Acute Lung Injury Caused by Paraquat Poisoning. *Oxidative medicine and cellular longevity***2019**, 1709718, doi:10.1155/2019/1709718 (2019).

27 Tai, W. *et al.* Rapamycin attenuates the paraquat-induced pulmonary fibrosis through activating Nrf2 pathway. *Journal of cellular physiology***235**, 1759-1768, doi:10.1002/jcp.29094 (2020).

28 Yang, C. *et al.* Spectrum of toxic hepatitis following intentional paraquat ingestion: analysis of 187 cases. *Liver international : official journal of the International Association for the Study of the Liver***32**, 1400-1406, doi:10.1111/j.1478-3231.2012.02829.x (2012).

29 Chen, G., Lin, J. & Huang, Y. Combined methylprednisolone and dexamethasone therapy for paraquat poisoning. *Critical care medicine***30**, 2584-2587, doi:10.1097/00003246-200211000-00030 (2002).

30 Huang, C. & Zhang, X. Prognostic significance of arterial blood gas analysis in the early evaluation of paraquat poisoning patients. *Clinical toxicology (Philadelphia, Pa.)***49**, 734-738, doi:10.3109/15563650.2011.607459 (2011).

31 Logan, S. & Storey, K. MicroRNA expression patterns in the brown fat of hibernating 13-lined ground squirrels. *Genomics*, doi:10.1016/j.ygeno.2021.01.017 (2021).

32 Gage, J. C. The action of paraquat and diquat on the respiration of liver cell fractions. *Biochem J***109**, 757-761, doi:10.1042/bj1090757 (1968).

33 Wright, G. & Reichenbecher, V. The effects of superoxide and the peripheral benzodiazepine receptor ligands on the mitochondrial processing of manganese-dependent superoxide dismutase. *Exp Cell*

*Res***246**, 443-450, doi:10.1006/excr.1998.4331 (1999).

34 Narasimhan, M. *et al.* Hydrogen peroxide responsive miR153 targets Nrf2/ARE cytoprotection in paraquat induced dopaminergic neurotoxicity. *Toxicology letters***228**, 179-191, doi:10.1016/j.toxlet.2014.05.020 (2014).

35 Wu, Y. *et al.* Caspase 3 is activated through caspase 8 instead of caspase 9 during H2O2-induced apoptosis in HeLa cells. *Cellular physiology and biochemistry : international journal of experimental cellular physiology, biochemistry, and pharmacology***27**, 539-546, doi:10.1159/000329955 (2011).

36 Beeraka, N. *et al.* The Taming of Nuclear Factor Erythroid-2-Related Factor-2 (Nrf2) Deglycation by Fructosamine-3-Kinase (FN3K)-Inhibitors-A Novel Strategy to Combat Cancers. *Cancers***13**, doi:10.3390/cancers13020281 (2021).

37 Shi, Z. *et al.* The LipoxinA4 receptor agonist BML-111 ameliorates intestinal disruption following acute pancreatitis through the Nrf2-regulated antioxidant pathway. *Free radical biology & medicine***163**, 379-391, doi:10.1016/j.freeradbiomed.2020.12.232 (2021).

38 Wang, T. *et al.* MSC-derived exosomes protect against oxidative stress-induced skin injury via adaptive regulation of the NRF2 defense system. *Biomaterials***257**, 120264, doi:10.1016/j.biomaterials.2020.120264 (2020).

39 Dudás, J., Ladányi, A., Ingruber, J., Steinbichler, T. B. & Riechelmann, H. Epithelial to Mesenchymal Transition: A Mechanism that Fuels Cancer Radio/Chemoresistance. *Cells***9** (2020).

40 Feng, R. *et al.* Nrf2 activation drive macrophages polarization and cancer cell epithelial-mesenchymal transition during interaction. *Cell communication and signaling : CCS***16**, 54, doi:10.1186/s12964-018-0262-x (2018).

41 Klein, S. *et al.* Endothelial responses of the alveolar barrier in vitro in a dose-controlled exposure to diesel exhaust particulate matter. *Particle and fibre toxicology***14**, 7, doi:10.1186/s12989-017-0186-4 (2017).

42 Chan, K. & Kan, Y. Nrf2 is essential for protection against acute pulmonary injury in mice. *Proceedings of the National Academy of Sciences of the United States of America***96**, 12731-12736, doi:10.1073/pnas.96.22.12731 (1999).

43 Hossain, K., Hosokawa, T., Saito, T. & Kurasaki, M. Amelioration of butylated hydroxytoluene against inorganic mercury induced cytotoxicity and mitochondrial apoptosis in PC12 cells via antioxidant effects. *Food and chemical toxicology : an international journal published for the British Industrial Biological Research Association***146**, 111819, doi:10.1016/j.fct.2020.111819 (2020).

44 Cui, P. *et al.* Human amnion-derived mesenchymal stem cells alleviate lung injury induced by white smoke inhalation in rats. *Stem cell research & therapy***9**, 101, doi:10.1186/s13287-018-0856-7 (2018).

Figures

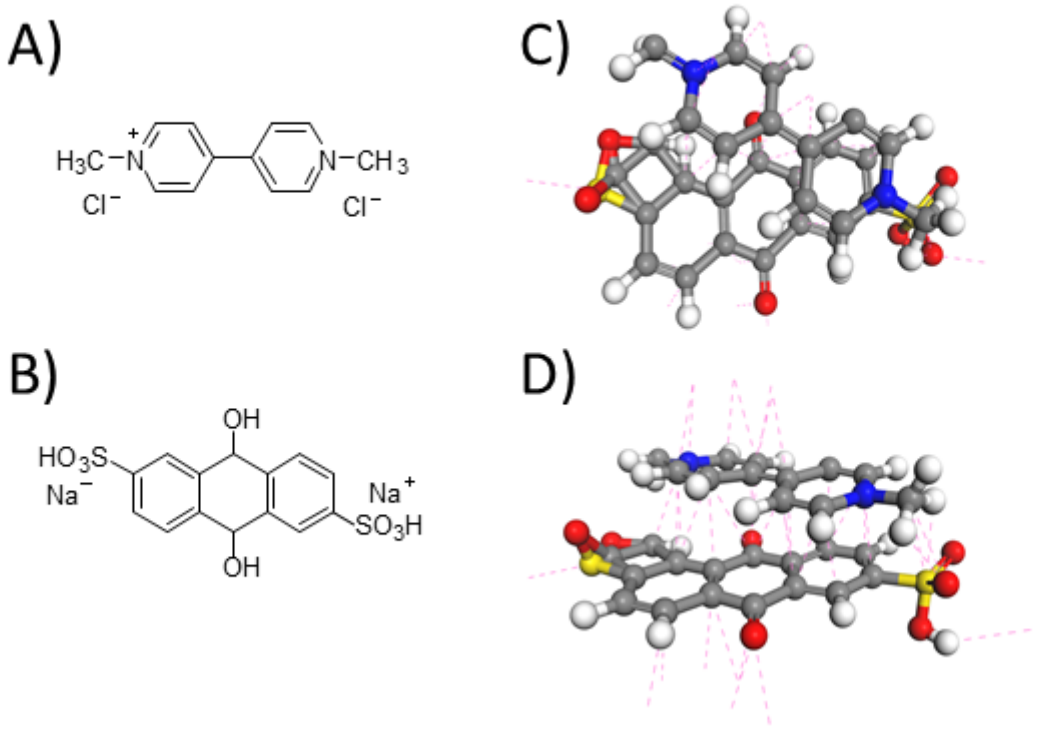

Figure 1

Complexation of PQ by AH2QDS. (A-B) Structures of PQ (A) and AH2QDS (B). (C-D) Complexes of PQ and AH2QDS by AutoDock Vina. C) is the side view and D) is the top view.

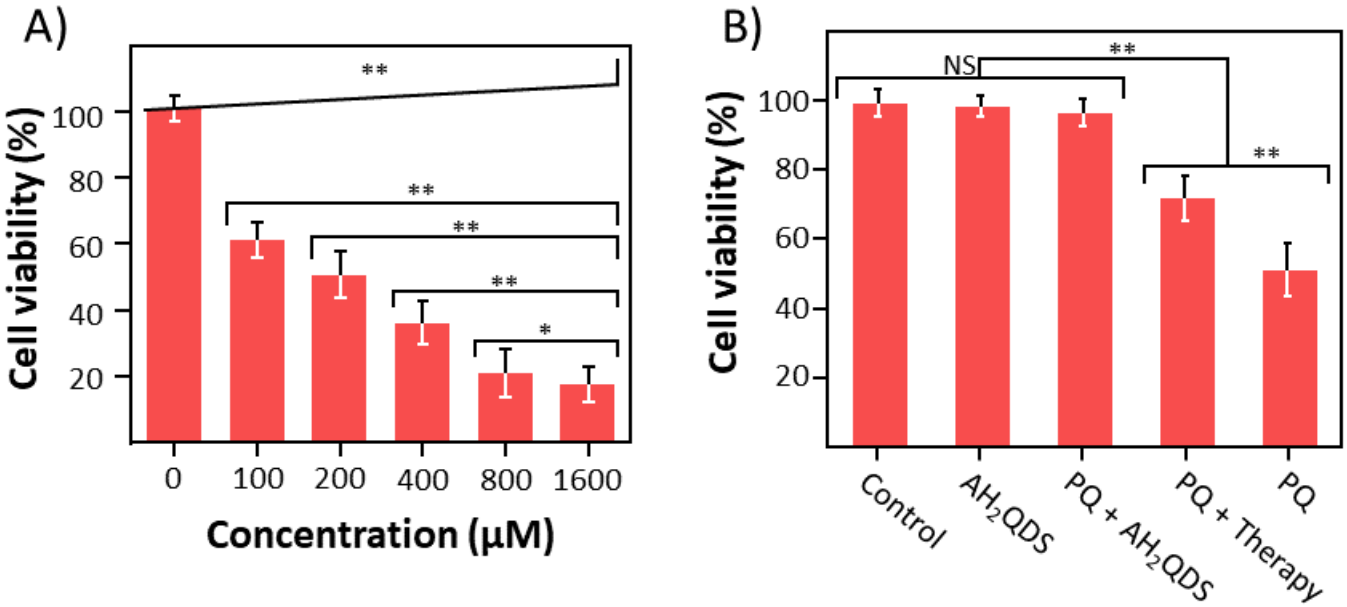

Figure 2

Antidotal effects of AH2QDS on PQ poisoning in vitro. (A) Changes in cell viability after 72h of treatment of A549 cells with different concentrations of PQ. (B)Effects of different treatment groups on the survival rate of A549 cells. Control group, without any treatment. In the AH2QDS group, A549 cells were incubated with 200 μM AH2QDS. In PQ + AH2QDS group, A549 cells were incubated with 200 μM PQ and 200 μM AH2QDS. A549 cells were incubated with 200 μM PQ and 200 μM glutathione in PQ + Therapy group. In the PQ group, A549 cells were incubated with 200 μM PQ. Data are presented as means ± SEM, n = 3, NS = not significant, *P<0.05, **P<0.001.

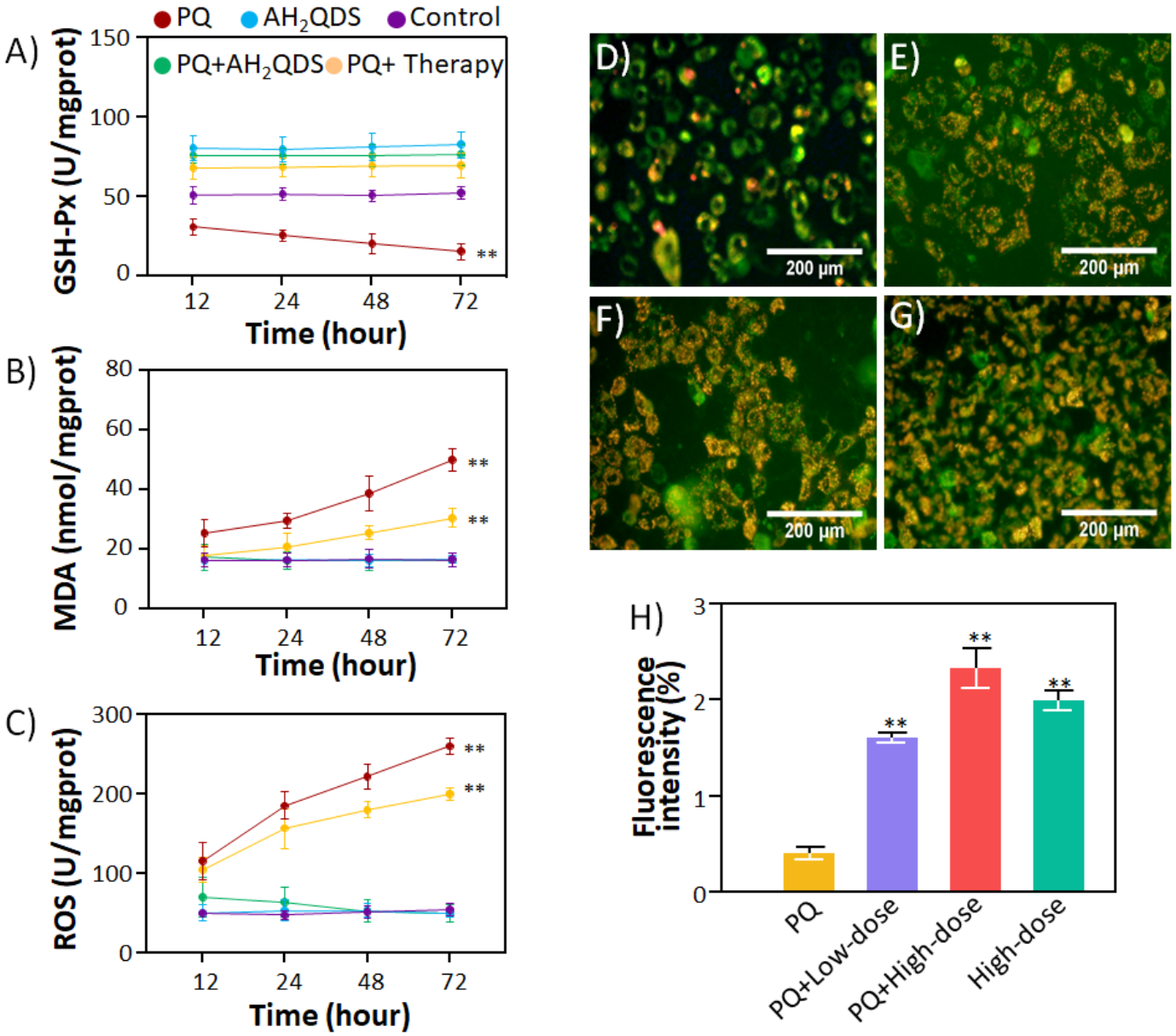

Figure 3

AH2QDS can protect the function of mitochondria and improve antioxidation in the treatment of PQ poisoning in vitro. (A-C) The levels of GSH-Px, MDA, and ROS were detected in different treatment groups. (D-G) The mitochondrial membrane potential of A549 cells in different treatment groups was detected. When the mitochondrial membrane potential is high, it can produce red fluorescence, and on the contrary, when the level of mitochondrial membrane potential is low, it can show green fluorescence. D) is the PQ group, A549 cells were incubated with 200 μm PQ. E shows PQ + Low-dose group, A549 cells were incubated with 200 μM PQ and 100 μM AH2QDS. F represents PQ + High-dose group, A549 cells were incubated with 200 μM PQ and 200 μM AH2QDS. G means that in the High-dose group, A549 cells were incubated with only 200 μM AH2QDS. (H) The value of mitochondrial membrane potential was obtained from the fluorescence ratio of red light to green light. Data are presented as means ± SEM, n = 3, *P<0.05, **P<0.001.

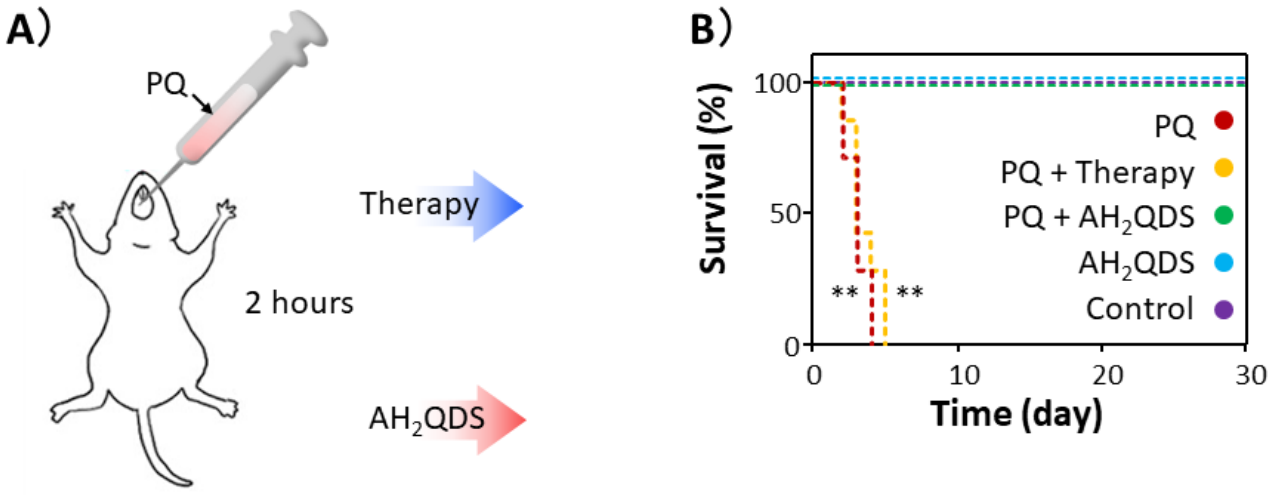

Figure 4

AH2QDS can improve the survival rate of rats poisoned by an ultra-lethal dose of PQ. (A) Scheme describing the administration ways. (B) The survival curve of rats in different treatment groups. The Control group served as blank control. In the AH2QDS group, only 400 mg/kg AH2QDS antidote was given by intragastric administration. In the PQ group, only PQ with 400 mg/kg concentration was given intragastrically. In the PQ + Therapy group, 400 mg/kg of PQ was given by intragastric administration first, and 500 mg/kg was given by intragastric administration 2 hours later, with a "white and black" scheme. In the PQ + AH2QDS group, 400 mg/kg of PQ was given to the stomach first, and 400 mg/kg of AH2QDS antidote was given 2 hours later. Kaplan-Meier survival analysis was used to analyze the survival rate of rats in different treatment groups, n = 7, *P<0.05, **P<0.001

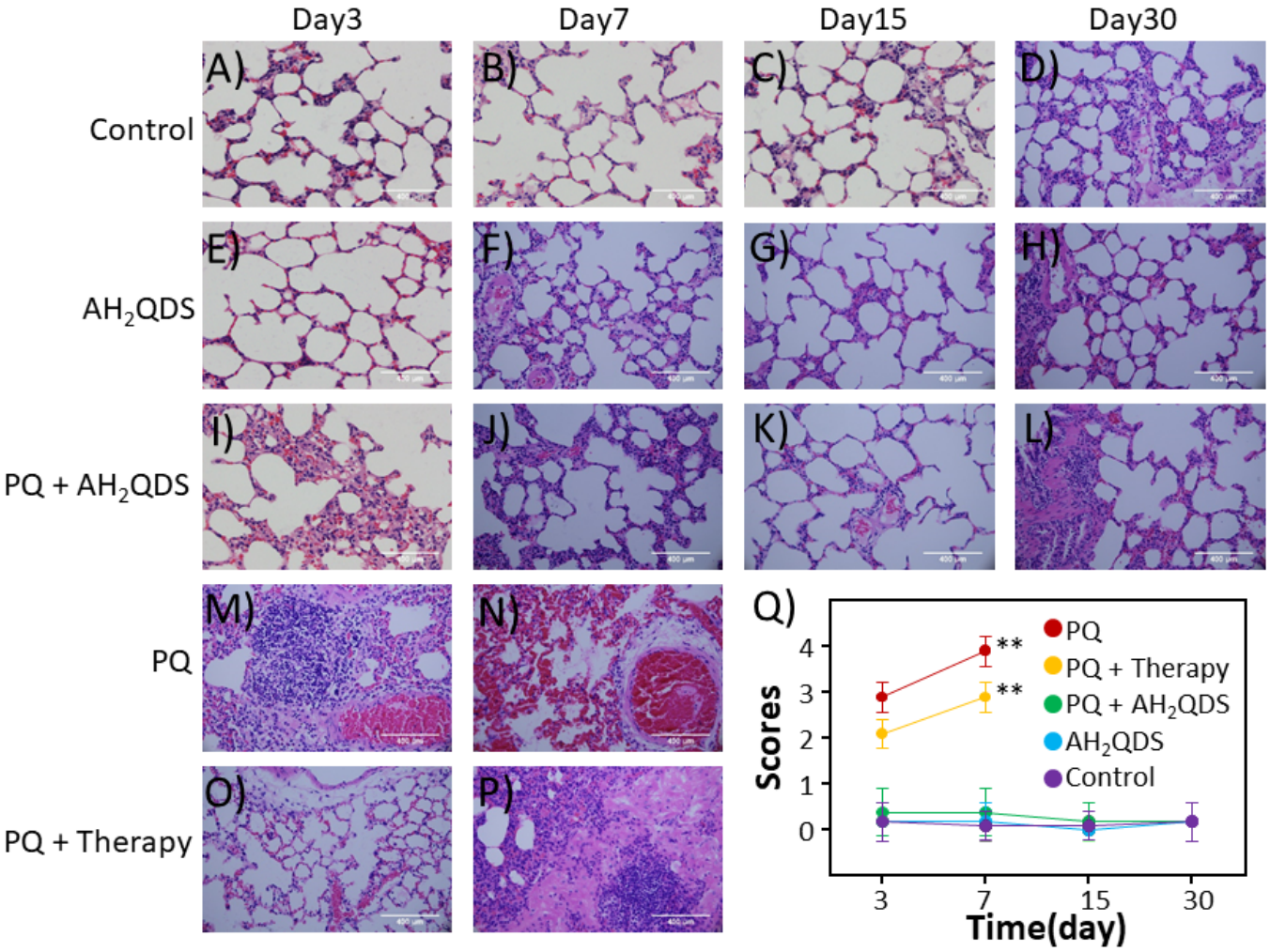

Figure 5

AH2QDS decreases lung injury. (A-P) H&E staining in lung tissue of rats in the diverse groups at different time points. (A-D) The Control group. (E-H) The AH2QDS group. (I-L) The PQ + AH2QDS group. (M-N) The PQ group. (O-P) The PQ + Therapy group. Due to PQ's super-lethal dose, rats in the PQ group and PQ + Therapy group died within one week, so there is no data for subsequent time points. (Q) Lung injury scores of different treatment groups. Data are presented as means ± SEM, n = 3, *P<0.05, **P<0.001.

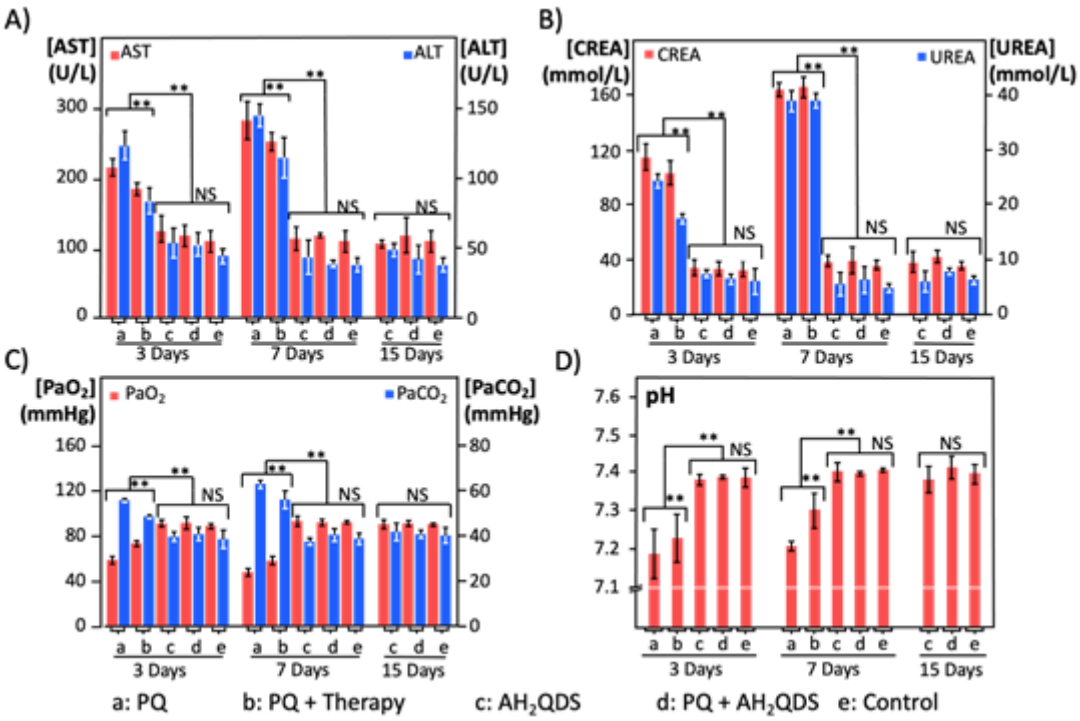

Figure 6

AH2QDS can reduce the damage of multiple organs and individual functions. (A-B) Changes in liver and kidney function of rats in each group. (C-D) Changes in blood gas analysis results of rats in each group. Due to a super-lethal dose of PQ intervention, animals in the PQ group and PQ + Therapy group died within one week, so there is no subsequent time point data. At 30 days, all groups' liver and kidney function and blood gas results were in the normal range. Data are presented as means ± SEM, n = 3, NS = not significant, *P<0.05, **P<0.001.

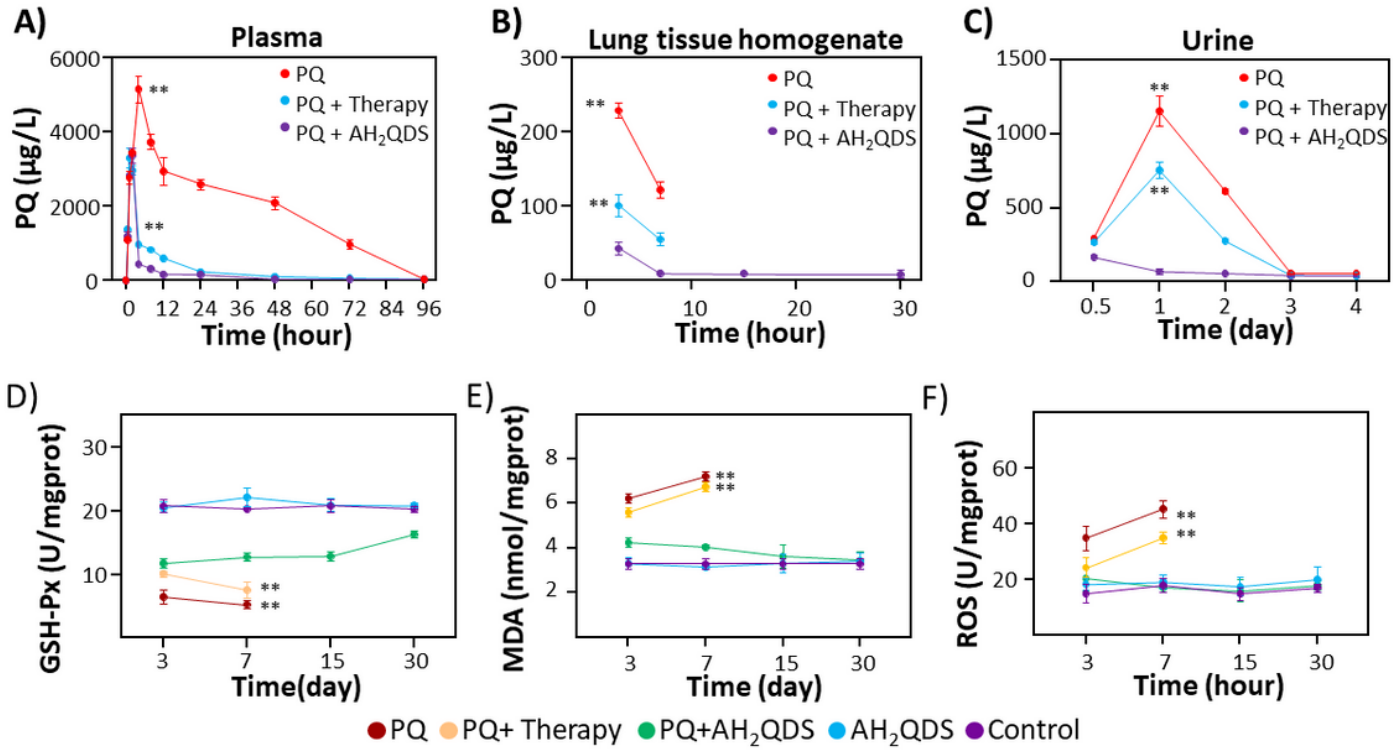

Figure 7

AH2QDS can reduce the drug concentration of PQ in vivo and improve the ability of antioxidant stress. (A-C) The concentration of PQ in plasma, tissue and urine was detected by Ultra high-performance liquid chromatography-tandem mass spectrometry. (D-F) The levels of GSH-Px, MDA, and ROS were detected in different treatment groups. Due to a super-lethal dose of PQ intervention, animals in the PQ group and PQ + Therapy group died within one week, so there is no subsequent time point data. Data are presented as means ± SEM, n = 3, *P<0.05, **P<0.001.

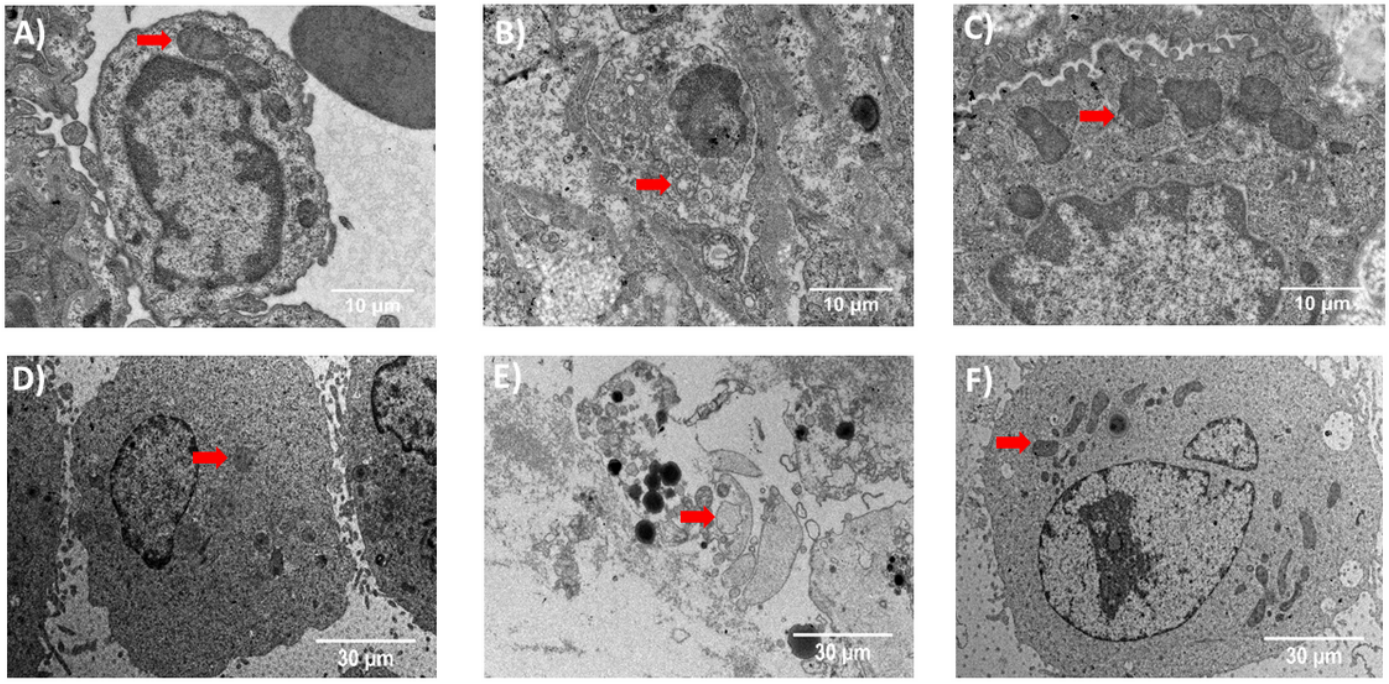

Figure 8

AH2QDS can protect the structural integrity of mitochondria. (A-C) The transmission electron microscope observed the structure of mitochondria in lung tissue. A) was the blank control group. B) was the PQ group, which was perfused with PQ of 400mg/kg concentration. C) was the PQ + AH2QDS group treated with a PQ of 400mg/kg concentration and then detoxified with AH2QDS of 400mg/kg concentration 2 hours later. (D-F) The transmission electron microscope observed the mitochondrial structure of A549 cells. D) was the blank control group. E) was PQ group, and A549 cells were treated with 200 μM PQ. F) was the PQ + AH2QDS group, A549 cells were incubated with 200 μM PQ and 200μM AH2QDS. The mitochondria have been marked with red arrows in the picture.

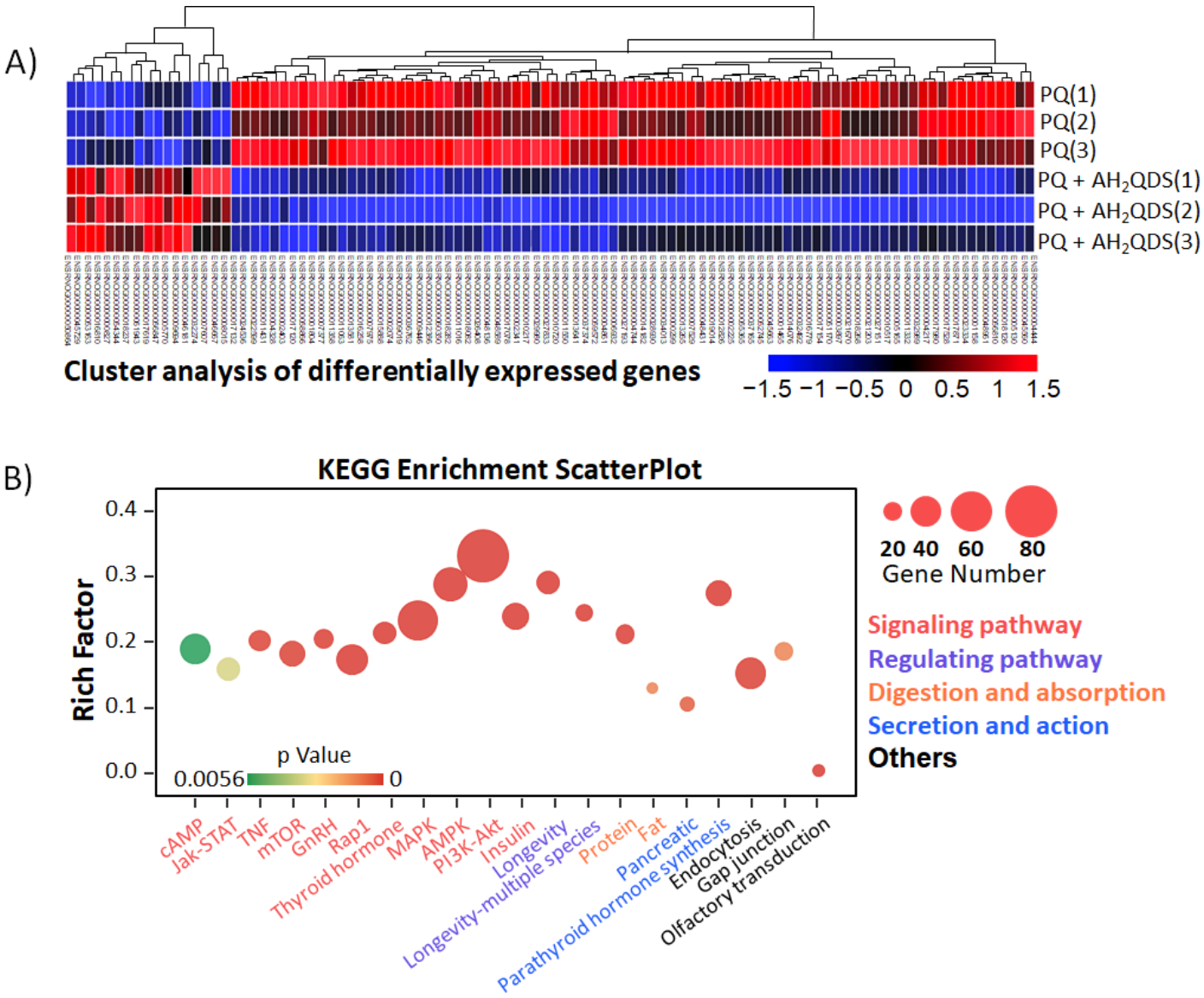

Figure 9

Differentially expressed genes by using RNA-sequencing method. (A) Heat map of differentially expressed gene expression profiles of the PQ group and the PQ + AH2QDS group. Gene enrichment analysis was performed based on differentially expressed genes, and the blue to red color indicates the expression level from low to high. (B) Regulatory biological pathways under AH2QDS treatment were analyzed using the KEGG database.

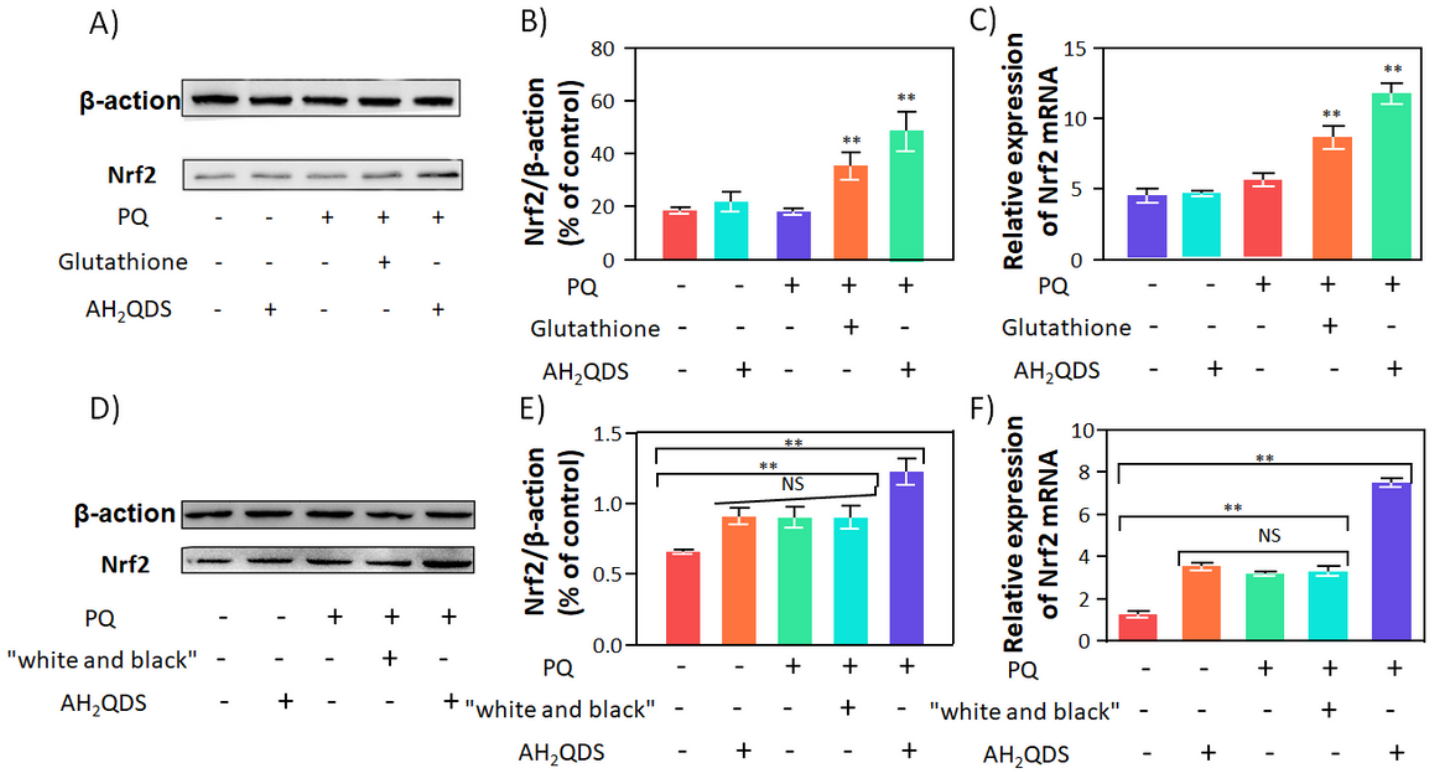

Figure 10

AH2QDS up regulated the expression of Nrf2. (A-C) After AH2QDS intervention, the expression of Nrf2 in A549 cells increased significantly. (D-F) The expression of Nrf2 in the lung tissue of rats detoxified by AH2QDS enhanced significantly. The grouping of gels/blots cropped from different parts of the same gel. Data are presented as means ± SEM, n = 3, NS = not significant, *P<0.05, **P<0.001.

Supplementary Files

This is a list of supplementary files associated with this preprint. Click to download.

- SupplementaryMaterial.docx
- table.docx
- FigS1.png
- FigS2.png
- FigS3.png
- FigS4.png